



## Quantitative reconstructions of mid- to late holocene climate and vegetation in the north-eastern altai mountains recorded in lake teletskoye



Natalia Rudaya<sup>a,b,c,d,\*</sup>, Larisa Nazarova<sup>d,e</sup>, Elena Novenko<sup>f,g</sup>, Andrei Andreev<sup>d,h</sup>, Ivan Kalugin<sup>i</sup>, Andrei Daryin<sup>i</sup>, Valery Babich<sup>i</sup>, Hong-Chun Li<sup>j</sup>, Pavel Shilov<sup>f</sup>

<sup>a</sup> Institute of Archaeology and Ethnography SB RAS, Ak. Lavrentieva Str. 17, 630090 Novosibirsk, Russia

<sup>b</sup> Novosibirsk State University, Pirogova Str. 2, 630090 Novosibirsk, Russia

<sup>c</sup> Altai State University, Dimitrova Str. 66, 656049 Barnaul, Russia

<sup>d</sup> Kazan Federal University, Kremlevskaya Str. 18, 420008 Kazan, Russia

<sup>e</sup> University of Potsdam, Institute of Earth and Environmental Science, Karl Liebknecht Str. 24-25, 14476 Potsdam, Germany

<sup>f</sup> Department of Geography, Moscow State University, Vorobievsky Gory 1, 119991 Moscow, Russia

<sup>g</sup> Institute of Geography Russian Academy of Science, Staromonetny lane, 29, 119017 Moscow, Russia

<sup>h</sup> Institute for Geology and Mineralogy, University of Cologne, Zùlpicher Str. 49a, 50674 Cologne, Germany

<sup>i</sup> Sobolev Institute of Geology and Mineralogy SB RAS, Ak. Koptyuga Str. 3, 630090 Novosibirsk, Russia

<sup>j</sup> Department of Geosciences, National Taiwan University, Taipei 106, Taiwan, ROC

### ARTICLE INFO

#### Article history:

Received 7 August 2015

Received in revised form 16 March 2016

Accepted 4 April 2016

Available online 19 April 2016

#### Keywords:

Mid-late Holocene

Siberia

Altai

Pollen

Climate

Vegetation

Transfer function

Woody coverage

### ABSTRACT

We report the first high-resolution (20–50 years) mid- to late Holocene pollen records from Lake Teletskoye, the largest lake in the Altai Mountains, in south-eastern West Siberia. Generally, the mid- to late Holocene (the last 4250 years) vegetation of the north-eastern Altai, as recorded in two studied sediment cores, is characterised by Siberian pine–spruce–fir forests that are similar to those of the present day. A relatively cool and dry interval with July temperatures lower than those of today occurred between 3.9 and 3.6 ka BP. The widespread distribution of open, steppe-like communities with *Artemisia*, Chenopodiaceae and Cyperaceae reflects maximum deforestation during this interval. After ca. 3.5 ka BP, the coniferous mountain taiga spread significantly, with maximum woody coverage and taiga biome scores between ca. 2.7 and 1.6 ka BP. This coincides well with the highest July temperature (approximately 1 °C higher than today) intervals. A short period of cooling about 1.3–1.4 ka BP could have been triggered by the increased volcanic activity recorded across the Northern Hemisphere. A new period of cooling started around 1100–1150 CE, with the minimum July temperatures occurring between 1450 and 1800 CE.

© 2016 Elsevier B.V. All rights reserved.

### 1. Introduction

The Altai Mountains provide an important connection between the Central Asian steppe and the North Asian forest-steppe. Holocene environmental changes might have had a significant influence on the development of human societies in this region. Many well-known archaeological sites from the Paleolithic to the Middle Ages, such as Denisova Cave, the Pazyryk necropolis, and the Ukok tombs, are situated in the Altai Mountains (Polosmak, 2001; Derevianko et al., 2003). The

Altai, which is shared by China, Kazakhstan, Mongolia and Russia is a prominent sub-longitudinal mountain range of Central Asia that extends approximately 1200 km in a north–south direction and rises up to 4500 m a.s.l. (Atlas of geological maps of Central Asia and adjacent areas, 2008). It is an important climatic and natural boundary at the limits of both Pacific and Atlantic influences and a divide between Boreal and Ancient Mediterranean floristic sub-kingdoms of the Holarctic (Takhhtajan, 1986). The Altai Mountains also contain relic vegetation types and paleoenvironmental studies can shed light on the vegetation history of the region. This is important, because a sizeable part of the Altai, including Lake Teletskoye, is a UNESCO World Heritage site, named the “Golden Mountains of Altai” (<http://whc.unesco.org/en/list/>).

Pollen records represent one of the most powerful tools to understand past environmental changes. Several Holocene pollen records from the Altai Mountains with varying time resolutions have been

\* Corresponding author at: Institute of Archaeology and Ethnography SB RAS, Ak. Lavrentieva Str. 17, 630090 Novosibirsk, Russia.

E-mail addresses: [nrudaya@gmail.com](mailto:nrudaya@gmail.com) (N. Rudaya), [larisa.nazarova@awi.de](mailto:larisa.nazarova@awi.de) (L. Nazarova), [lananov@mail.ru](mailto:lananov@mail.ru) (E. Novenko), [aandreev@uni-koeln.de](mailto:aandreev@uni-koeln.de) (A. Andreev), [ikalugin@igm.nsc.ru](mailto:ikalugin@igm.nsc.ru) (I. Kalugin), [avd@uigm.nsc.ru](mailto:avd@uigm.nsc.ru) (A. Daryin), [vbabich@igm.nsc.ru](mailto:vbabich@igm.nsc.ru) (V. Babich), [hcli1960@ntu.edu.tw](mailto:hcli1960@ntu.edu.tw) (H.-C. Li), [www.stromboli@mail.ru](mailto:www.stromboli@mail.ru) (P. Shilov).

published in recent decades (Gunin et al., 1999; Tarasov et al., 2000; Blyakharchuk et al., 2004, 2007, 2008; Andreev et al., 2007; Schlütz, Lehmkuhl, 2007; Rudaya et al., 2009, 2012). However, these records and their resolutions are insufficient for detailed palaeoenvironmental reconstructions, taking into account the size and heterogeneity of the territory.

Here, we report on the first high-resolution (20–50 years) mid- to late Holocene pollen records from Lake Teletskoye, obtained from the underwater Sofia Lepneva Ridge in 2006 (core Tel 2006) and from the deepest part of the lake in 2001 and 2004 (combined core Tel 2001–2004). The uppermost part of the Tel 2001–2004 core was palynologically examined by Andreev et al. (2007), but was never used for quantitative reconstructions. In addition to taxonomy, newly developed statistical approaches strengthen the use of pollen data and allow numerical reconstructions of climate parameters. This paper presents (i) the results of palynological analysis of the cores; and (ii) quantitative reconstructions of the late-Holocene regional vegetation, woody coverage and climate. Regional comparisons were performed, to infer the paleoenvironmental and paleoclimatic history of this poorly documented region. These new results lead to a better understanding of the role of the northeastern Altai in the Holocene environmental history of Central Asia.

## 2. Regional setting

The northeastern Altai (51–52°N, 86–88°E) is an extensive plateau with isolated massifs of approximately 2000 m a.s.l. that are bisected by deep river valleys (Kuminova, 1960). The region possesses a unique evergreen coniferous taiga that is dominated by Siberian fir and Siberian pine, as well as deciduous trees and some relic herbaceous species. The vegetation in the region is floristically close to the Subatlantic type of European hemiboreal forests (Ermakov, 2003). Despite significant afforestation, the region is classified within the Holarctic zone of the Eurasian steppe (Lavrenko, 2000). The montane forest belt of the Altai Mountains

connects to the taiga zone of Siberia via forests of the Kuznetsky Alatau, a part of the Sayan Mountains.

Lake Teletskoye (spanning 51°20' to 51°47'N and 87°15' to 87°50'E) is the largest lake in the Altai Mountains (Figs. 1A, 2) and is 77 km long and 330 m deep and filled by approximately 40 m of sediments. The lake appeared by the end of the Late Pleistocene, when water filled a tectonic depression (Selezneev et al., 1995). Lacustrine and alluvial deposits in the southeastern part of the lake (Bele terrace located above the modern lake level) were radiocarbon-dated to 27,060 ± 850 ka BP. These are the oldest known lacustrine sediments in the lake basin (Rusanov and Orlova, 2013). The Chulyshman River, one of the largest rivers of the Russian Altai, flows into the lake from the south and drains 84% of the lake catchment area. Several smaller rivers also flow into the lake. The Biya River flows out of the lake to the north (Selegei and Selegei, 1978). The altitude of the mountains surrounding the lake is 1900 m a.s.l. on average. Due to the lake's influence, the climate of the basin is relatively mild, especially in the south. The mean annual temperatures of 3.2–4.0°C are approximately 1 °C higher than in other regions surrounding the lake (<http://wcatlas.iwmi.org>). The mean January temperatures are about –8.5 °C, and mean July temperatures are approximately 17.5 °C (data from the Yailu weather station). The mean annual precipitation varies between 822 mm/yr in the north and 460 mm/yr in the south (Kuminova, 1960).

As this north-eastern part of the Altai Mountains is characterised by higher annual precipitation, it results in the absence of the steppe belt that occurs, at least fragmentarily, in other parts of the mountains (Kuminova, 1960). Only very small patches along the lakeshore represent steppe-like vegetation. Birch forests mixed with meadows occur at lower altitudes, up to 700 m a.s.l. Unique evergreen (so-called 'dark') coniferous forest with dominating Siberian fir (*Abies sibirica*), aspen (*Populus tremula*), dense understory with bird cherry (*Padus avium*), mountain ash (*Sorbus sibirica*), viburnum (*Viburnum opulus*) and a number of relic herbaceous species such as *Dryopteris filix-mas*, *Brachypodium sylvaticum*, *Festuca gigantea*, *Poa remota*, *Asarum*

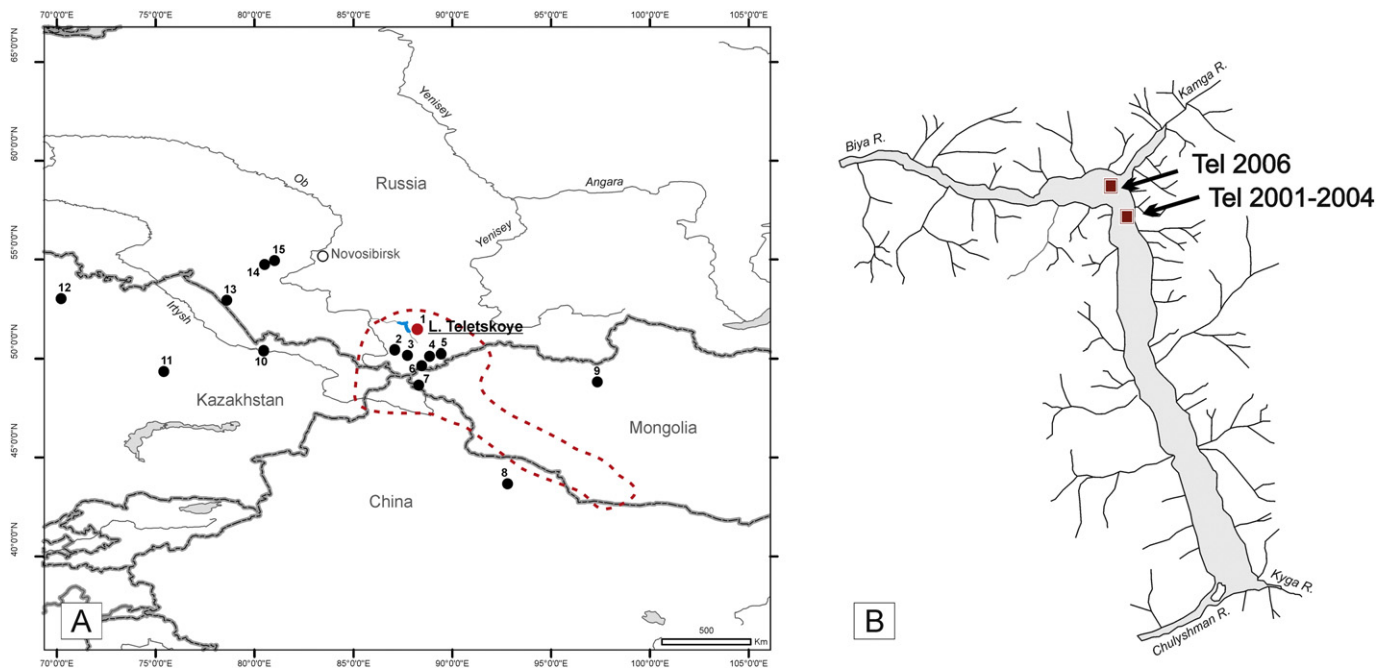


**Fig. 1.** A. Map of the study area and summary chart showing the distribution of the mid-late-Holocene palaeoclimate records from Altai Mountains and the neighboring regions discussed in the text: 1. Lake Teletskoye (51°35'N, 87°40'E; this study), 2. Lake Uzun-Kol (50°29'00"N, 87°6'30"E; Blyakharchuk et al., 2004), 3. Lake Dzhangskol (50°11'N, 87°44'E; Blyakharchuk et al., 2008), 4. Kuray Range (50°08'04"N, 88°51'10"E; Schlütz and Lehmkuhl, 2007), 5. Lake Ak-Kol (50°15'N, 89°37'30"E; Blyakharchuk et al., 2007), 6. Tarkhata Valley (49°39'01"N, 88°28'10"E; Schlütz and Lehmkuhl, 2007), 7. Hoton-Nur Lake (48°40'N, 88°18'E; Rudaya et al., 2009), 8. Lake Bakikun (An et al., 2011), 9. Telmen Lake (Peck et al., 2002), 10. Ozerki Swamp (50°24'N, 80°28'E; Kremenetski et al., 1997), 11. Pashennoe Lake (49°22'N, 75°24'E; Kremenetski et al., 1997), 12. Lake Karasye (53°02'N, 70°13'E; Kremenetski et al., 1997), 13. Lake Big Yarovoe (52°51.156'N, 78°37.601'E; Rudaya et al., 2012), 14. Suminskoye Zaimitsche (54°45'N; 80°31'E; Klimanov et al., 1987), 15. Kayakskoye Zaimitsche (54°57' N; 81°01' E; Levina et al., 1987). Dashed line is contour of Altai Mountains. B. Lake Teletskoye with the core locations marked and associated hydrological network.

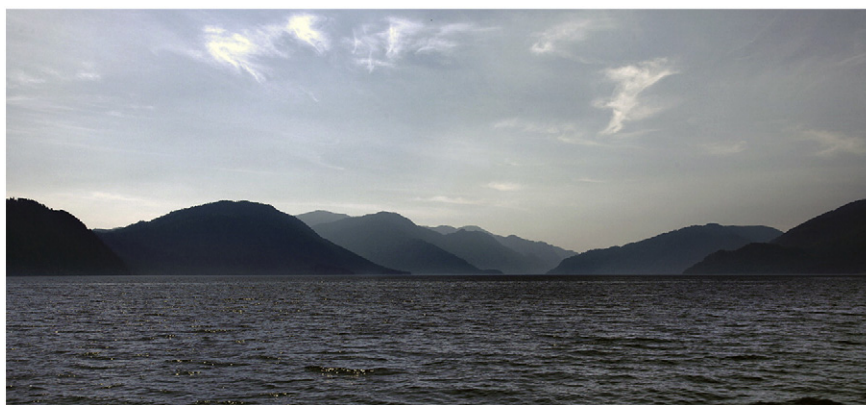


Fig. 2. Dark coniferous forest around Lake Teletskoye (photo by Alexey Ebel).

*europaeum* and *Stachys sylvatica*, grow between 700 and 1700 m a.s.l. The mountains above 1700 m are covered by Siberian pine (*Pinus sibirica*) forest. Above the tree line, at about 1800 m, alpine tundra and alpine meadow communities are widespread (Kuminova, 1960). According to the VCF data (Vegetation Continuous Fields product; Hansen et al., 2003), the modern woody cover in a 20-km zone around the lake reaches approximately 55% (<http://glcf.umiacs.umd.edu/data/vcf>).

Notably, the territory around the lake is under government protection and any human activities there are prohibited. Except for Bronze Age settlements in the non-forested Chulyshman River valley, no historical or archaeological evidence of human settlements in the vicinity of the lake exist. This essentially makes Lake Teletskoye a unique location in which to investigate the undisturbed environmental history of the Altai Mountains.

### 3. Data and methods

#### 3.1. Coring and age-depth model

A 110-cm-long sediment core was obtained by a 60-mm gravity corer in 2001. The core location (51°43'N, 87°39'E) was at a water depth of 330 m at the deepest part of the lake. The uppermost 20 cm of the sediments was additionally collected using a Wildco box corer. The 2001 core was combined with another core obtained in the same place in 2004, based on the characteristic sediment lamination and magnetic susceptibility at a depth of 90 cm. The length of the combined core Tel 2001–2004 is 173 cm. The sediment core consists of bluish-grey to dark-green finely laminated clays and silts and shows undisturbed, horizontal layers without any traces of bioturbation. The sediments between 99 and 89 cm depth include a 10-cm-thick sand-rich layer, which possibly is a turbidite (Kalugin et al., 2007).

The age-depth model for the combined core Tel 2001–2004 (Fig. 3C) is based on two radiocarbon dates obtained from wood fragment and remains of moss (Table 1), and the  $^{137}\text{Cs}$  content, and was constructed with the Bacon 2.2 package (Blaauw and Christen, 2011) of R software (R Core Team, 2012). The average sedimentation rate, based on changes in the  $^{137}\text{Cs}$  and  $^{210}\text{Pb}$  contents, was previously estimated as 1.125 mm/yr (Kalugin et al., 2005; Andreev et al., 2007).

In 2006, the 194-cm-long sediment core Tel 2006 was recovered from the underwater Sofia Lepneva Ridge in the northern part of Lake Teletskoye (51°44.99'N, 87°37.414'E, Fig. 1B). The depth at the coring site was approximately 90 m. The coring was performed with a 100-mm gravity corer equipped with a blade catcher. The sediment core Tel 2006 consists of bluish-grey to dark-green finely laminated clays and silts. The core shows undisturbed horizontal layers (varves) without any traces of bioturbation.

Sixteen bulk sediment samples from the Tel 2006 core were AMS-dated (Table 1, Fig. 3A). Total organic carbon (TOC) was used for dating

because of the absence of plant macrofossils in the sediments, although the bulk TOC is not ideal for  $^{14}\text{C}$  dating, as it can contain carbon from different sources that is not syndepositional in age (Colman et al., 1996; Zhou et al., 2015). The age-depth distribution of  $^{14}\text{C}$  dates from the Tel 2006 core suggests contamination of the sediments by old carbon (Fig. 3A). This effect is well known and has been described for the large lakes in different parts of the world (e.g., Moreton et al., 2004; Prokopenko et al., 2007; Watanabe et al., 2009; Zhou et al., 2015).

To obtain a more reliable chronology, the  $^{210}\text{Pb}$  activity and  $^{137}\text{Cs}$  content were also analysed (Kalugin et al., 2009). The measurement points were converted into units of time based on estimates of the sediment accumulation rate by the isotope dating. The value obtained for the mean linear rate of dry matter accumulation equal to 0.45 mm per year, was used to create the chronology. The peak of  $^{137}\text{Cs}$  was assigned to 1963 CE (atmospheric testing of nuclear weapon) at the core depth of 1.9 cm. The logarithmic distribution of  $^{210}\text{Pb}$  was performed to a depth of 48 mm (Fig. 3B).

A light layer observed at a depth of 38–39 cm in the Tel 2006 core (Fig. 3A) differs from the adjacent dark layers and has a higher Sr/Rb ratio (Kalugin et al., 2009), demonstrating a coarse-grained silt fraction and representing a coarse material influx event. According to the  $^{210}\text{Pb}$  age-depth model for Tel 2006, the sediments at 38–39 cm depth accumulated at about 0.789–0.811 cal ka BP. A similar marker layer exists in the Tel 2001–2004 core obtained from the deepest part of the lake (330 m), which was dated by AMS to  $895 \pm 45$   $^{14}\text{C}$  (765–891 cal) yr BP. As both age models coincide very well, we can suggest that this layer is correlative in both cores and can use it as a marker layer. This marker layer was also observed in several cores from the northern part of the lake and reflects a significant sedimentation event that affected the whole lake (Kalugin et al., 2005, 2007). According to our age-depth model based on the  $^{210}\text{Pb}$  accumulation rate and correlation of  $^{137}\text{Cs}$  peaks, the Tel 2006 core spans the last ~4.25 ka (Fig. 3A, B).

#### 3.2. Palynological method

A total of 105 samples from the Tel 2006 core and 64 samples from the Tel 2001–2004 cores, each consisting of 0.1–1.0 g of dry sediment taken every 2.5 cm on average, were prepared for pollen analysis using standard procedures (Faegri and Iversen, 1989). *Lycopodium* spore tablets were added to each sample to calculate the total pollen and spore concentration. Pollen grains mounted in glycerin were analysed under a light microscope with 400× magnification. Additionally, coniferous stomata and other non-pollen palynomorphs (NPPs) were also counted on pollen slides. Microscopic analysis revealed high pollen concentrations and a good preservation of pollen grains, allowing of a minimum of 300 terrestrial pollen grains per sample to be counted. Pollen percentages were calculated based on a pollen sum of all pollen and spore taxa, taken as 100%. The results of the pollen analysis are



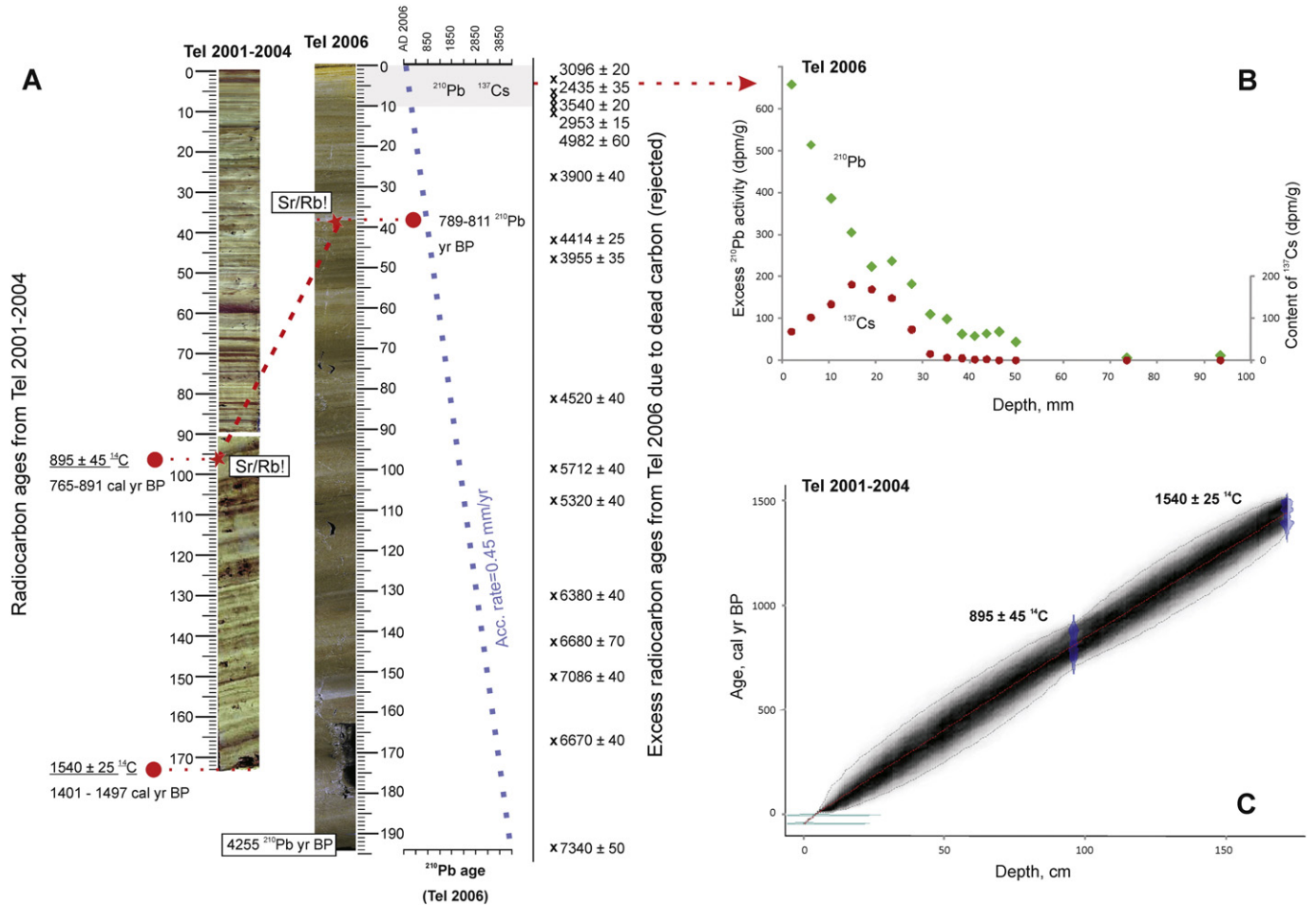


**Fig. 3.** A. Tel 2001–2004 and Tel 2006 cores with identical lithology illustrating problematic radiocarbon ages due to abundant dead carbon and <sup>210</sup>Pb based age-depth model for the core Tel 2006. B. Excess <sup>210</sup>Pb activity and <sup>137</sup>Cs content in upper 100 cm of core Tel 2006. C. Age-depth model for the core Tel 2001–2004 (detailed description of age-depth model in the text).

displayed in pollen diagrams (Figs. 4A, 5A), produced using Tilia 1.7.16 software (Grimm, 2004). The definition of the local pollen zones is supported by CONISS (Grimm, 1987).

**Table 1**  
AMS dates from the Tel 2001–2004 and Tel 2006 cores presented in this study.

Lab code Sample ID	Dated material	Depth (cm)	Radiocarbon age ( <sup>14</sup> C yr BP)
<i>Tel 2006</i>			
NTUAMS-412	Bulk sediment	3.25	3096 ± 20
KIA26034	Bulk sediment	6	2435 ± 35
NTUAMS-413	Bulk sediment	7.25	3540 ± 20
NTUAMS-414	Bulk sediment	9.25	2953 ± 15
NTUAMS-415	Bulk sediment	10.55	4982 ± 60
Poz-34102	Bulk sediment	27	3900 ± 40
NTUAMS-416	Bulk sediment	42.25	4414 ± 25
Poz-34139	Bulk sediment	48.5	3955 ± 35
Poz-34104	Bulk sediment	82.5	4520 ± 40
NTUAMS-417	Bulk sediment	99.75	5712 ± 40
Poz-34140	Bulk sediment	112.5	5320 ± 40
NTUAMS-418	Bulk sediment	130.25	6380 ± 40
Poz-34141	Bulk sediment	142	6680 ± 70
NTUAMS-419	Bulk sediment	150.25	7086 ± 40
Poz-34143	Bulk sediment	166.5	6670 ± 40
Poz-34105	Bulk sediment	194	7340 ± 50
<i>Tel 2001–2004</i>			
KIA26018	Remains of moss	96.5	895 ± 45
KIA29870	wood fragment	173	1540 ± 25

### 3.3. Biomisation

Biome reconstruction (so-called biomisation) was accomplished via a quantitative approach that uses fuzzy logic introduced by Prentice et al. (1996). The method is based on an objective assignment of pollen taxa to plant functional types (PFTs) on the basis of modern ecology, bioclimatic tolerance and the geographical distribution of pollen-producing plants (Box, 1996). Taxa can be assigned to more than one PFT, because they include species from various ecosystems. The plant functional types are combined to form biomes. A particular biome is characterised by a particular set of PFTs. Finally, a taxon-biome matrix is formed, in which each pollen taxon is correlated with one or several biomes. In this study, we used a taxon-biome matrix and a calculation equation in which 47 pollen taxa were attributed to 10 biomes that occur in Northern Eurasia. This method applied to 51 surface pollen spectra from the Altai region (including mountainous areas) assigned 71% of the samples to the correct biome (Rudaya, 2013).

### 3.4. Past woody coverage estimation

The method used for woody cover reconstructions combines modern and fossil pollen records and satellite-based tree cover data (Hansen et al., 2003) with the best modern analogue (BMA) approach (Overpeck et al., 1985; Guiot, 1990), which is based on searching for the closest analogues of fossil spectra among the modern dataset. The method was recently applied to pollen spectra from Northern Eurasia (e.g., Tarasov et al., 2007 and references therein) and the European

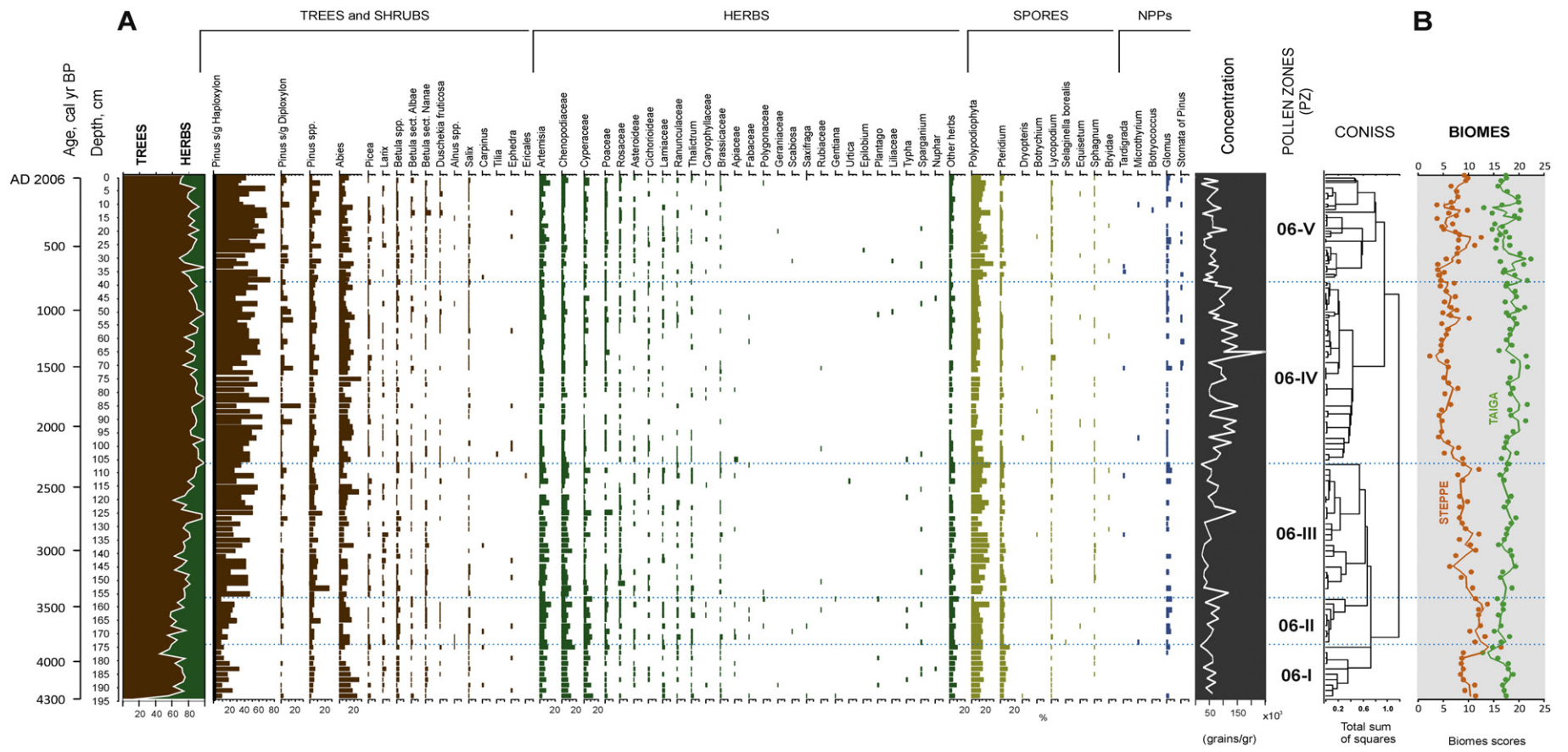


Fig. 4. Tel 2006 pollen percentage diagram (A) and biome reconstruction (B).

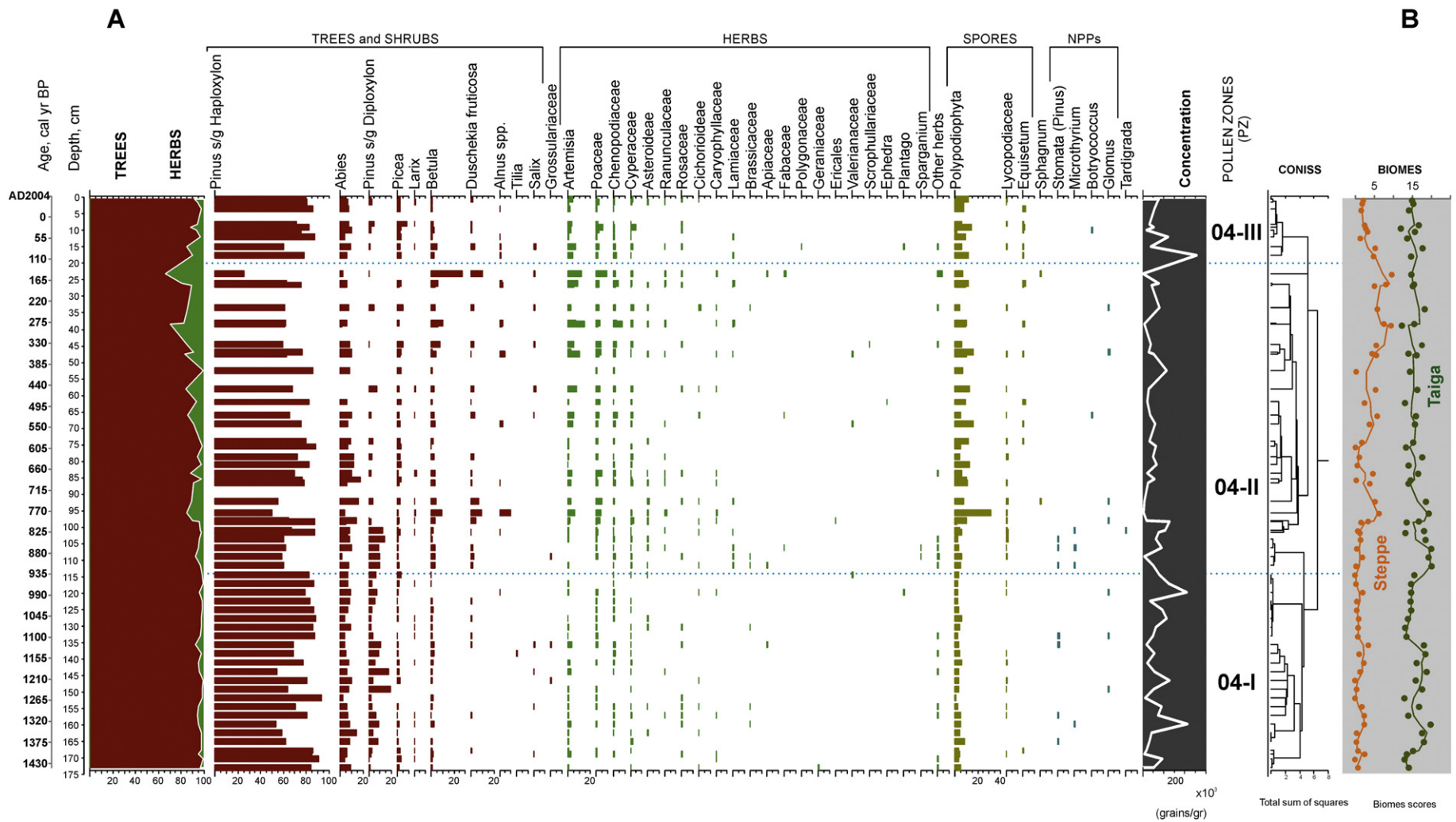


Fig. 5. Tel 2001–2004 pollen percentage diagram (A) and biome reconstruction (B).



part of Russia (Novenko et al., 2014), demonstrating that this technique can be very effective for reconstructing tree cover during the Late Pleistocene and Holocene.

The modern tree-cover estimates were taken from the VCF (Vegetation Continuous Fields) product (Hansen et al., 2003). The product is derived from observations of the MODerate-resolution Imaging Spectroradiometer (MODIS) carried onboard NASA's Terra satellite (<http://glcf.umiacs.umd.edu/data/vcf>). In this study, we used the VCF product collection 4, produced from MODIS observations in 2005. The proportion of forest land in 5-, 10-, 20-, and 50-km radii around each surface pollen site from a reference dataset was calculated by averaging the per-pixel MODIS estimates of tree cover.

To test the accuracy of regional woody cover reconstructions using the BMA approach, a leave-one-out cross-validation (ter Braak, 1995) was applied to the referenced modern dataset. In this study, we used a pollen dataset from a sizeable part of northern Asia (47°46'–73°66'N and 55°54'–133°13'E) that includes 204 modern surface pollen spectra. The modern pollen spectra were sequentially removed from the total modern dataset one at a time. For each removed pollen spectrum, the total woody cover in different radii around the site was calculated on the basis of the remaining modern dataset by the BMA method. The results were then compared with the known value of woody cover around this site.

The leave-one-out cross-validation test showed the best correlation between pollen-based modern woody cover reconstructions and MODIS measurements at a radius of 20 km ( $R^2 = 0.5546$  and RMSEP = 11.8%), which is sufficient for the reconstruction of major changes in forest vegetation (Novenko et al., 2014). Accordingly, in this study, we used a distance of 20 km as a characteristic radius to reconstruct changes in woody coverage. It should be noted that the 20-km radius roughly corresponds to the pollen source area for small lakes and mires often studied by pollen analysts (Bradshaw and Webb, 1985). Even for large lakes, approximately 60% of pollen originates within a 25-km distance from the shore (Hellman et al., 2008).

### 3.5. Multivariate statistics for climate reconstruction

To develop a pollen-based inference model for quantifying past regional climate and environmental changes in Northeast Altai, we used the same reference pollen dataset as in the BMA approach for woody cover reconstruction. Pollen percentages were calculated on the basis of the total pollen sum. Only pollen taxa with a frequency of  $\geq 0.5\%$  in at least three samples were included in the numerical analyses (Wang et al., 2014) resulting in a reduction in the number of pollen taxa from 76 to 66.

The mean temperature of the warmest month (MTWA), the mean temperature of the coldest month (MTCO), the mean annual temperature (TANN), and the mean annual precipitation (PANN) are the environmental variables that presumably correlate with vegetation and pollen fluctuations. Modern air temperatures for each site were obtained from a climatic dataset compiled by New et al. (2002), measured at 2 m above the ground in standard meteorological screens. The New et al. (2002) dataset uses climatic norms from 1961 to 1990 to create a global climatic grid with a 10-min latitude/longitude resolution. Some shortcomings are associated with this dataset; for example, the relatively coarse resolution of climatic data and that the climate norms predate the collection of pollen data and span a cold phase of the Arctic Oscillation (Overland and Wang, 2005). However, the global nature of the New et al. (2002) dataset, as well as its homogeneity and consistency, make it more suitable for our purposes than data from local meteorological stations. The latter datasets have gaps in observations and cover different time spans. The PANN data were obtained from the SamSam water database (<http://www.samsamwater.com>).

Within the study area, the annual temperature range was based on the MTWA and MTCO. Apart from the MTCO, all environmental data were normally distributed. The skewness reflects the degree of

asymmetry of a data distribution around its mean. Normal distributions produce a skewness statistic of about zero. Values that exceeded 2 standard errors of skewness (regardless of sign) were classed as significantly skewed (Sokal and Rohlf, 1995). Apart from the MTCO, all environmental data were normally distributed. The MTCO data were  $\text{Log}_{10}$ -transformed for the analysis to normalise their distribution and to stabilise their variances (Birks, 1998).

Pollen percentages were square-root-transformed for the numerical analyses to stabilise variances and optimise the signal-to-noise ratio. Correspondence Analysis, detrended by segments, was performed on the pollen data to explore the main pattern of taxonomic variations among sites and to determine the lengths of the sampled environmental gradients, from which we decided whether unimodal or linear statistical techniques would be the most appropriate for the data analysis (Birks, 1995). Ter Braak and Prentice (1988) suggested that the length of the first major gradient of variation in multivariate biological data, as estimated by detrended correspondence analysis (DCA) (Hill and Gauch, 1980) (estimated in standard deviation (SD) units of turnover), is a useful guide as to whether species responses are primarily monotonic (gradient length  $< 2$  SD) or primarily unimodal (gradient length  $> 2$  SD). Such estimates of turnover along an environmental gradient are a guide to the type of regression procedure that should be used to develop calibration functions from modern calibration sets for quantitative environmental reconstructions (Birks, 1995, 1998; Birks, 2010; Juggins and Birks, 2012). The DCA axes 1 and 2 were 3.86 and 3.619 standard deviation units, respectively, indicating that numerical methods based on a unimodal response model are appropriate to assess the variation structure of pollen assemblages (ter Braak, 1995).

Variance inflation factors (VIF) were used to identify inter-correlated variables. Environmental variables with a VIF  $> 20$  were eliminated, beginning with the variable with the largest inflation factor, until all remaining variables had values  $< 20$  (ter Braak and Šmilauer, 2002a). The initial Canonical Correspondence Analyses (CCA) with four environmental variables showed that MTCO, MTWA and TANN were linked or intercorrelated; Therefore, TANN and MTCO were eliminated from the analysis.

Relationships between the pollen distribution and environmental variables were assessed using a set of CCA with each environmental variable as the sole constraining variable. The statistical significance of each variable was tested by a Monte Carlo permutation test with 999 unrestricted permutations (ter Braak, 1990). In this test, the ratio of the first constrained eigenvalue to the second unconstrained eigenvalue indicates the significance of the variable in explaining the cumulative variance in the taxon data. Inference models derived from explanatory variables with high ratios are therefore likely to have greater predictive power. Both DCA and CCA were performed using CANOCO 4.5 (ter Braak and Šmilauer, 2002b).

Quantitative transfer functions were developed using weighted averaging (WA) and weighted averaging partial least squares (WA-PLS) methods (Barley et al., 2006; ter Braak and Looman, 1986; ter Braak and Juggins, 1993). The performance of the models and optimal number of components in the transfer function were assessed using leave-one-out cross validation. Each inference model was evaluated using the coefficient of determination ( $r^2_{\text{Jack}}$ ), the root-mean-squared error of prediction (RMSEP), a measure of random error in the model (Altman and Bland, 1983) and the maximum biasjack (the tendency of the model to over- or underestimate the reconstructed value along a particular part of the gradient). Robust transfer functions were those that had the lowest RMSEP, a high coefficient of determination ( $r^2_{\text{Jack}}$ ) and a low mean and maximum biasjack. The number of components included in the final model was selected based on reducing the RMSEP by at least 5% (Birks, 1998). The program C2 version 1.5 (Juggins, 2007) was used to develop and assess the transfer functions.

Goodness-of-fit statistics derived from a canonical correspondence analysis (CCA) of the modern calibration data and down-core passive samples with MTWA as the sole constraining variable were used to

assess the fit of the analysed down-core assemblages to temperature (Birks et al., 1990; Birks, 1995, 1998). This method allows an assessment of how unusual the fossil assemblages are with respect to the composition of the training set samples along the temperature gradient. Fossil samples with a larger residual distance to the first CCA axis than the 90th and 95th percentile of the residual distances of all the modern samples were identified as samples with a 'poor fit' and a 'very poor fit' with MTWA, respectively (Birks et al., 1990). The CCA was performed using the program CANOCO 4.5 (ter Braak and Šmilauer, 2002b).

## 4. Results

### 4.1. Pollen analysis, biomisation and woody coverage

#### 4.1.1. Tel 2006

In total, 51 pollen and spore taxa were identified in the Tel 2006 core. The Tel 2006 pollen diagram (Fig. 4A) is subdivided into five pollen zones (PZs) on the basis of changing pollen taxa composition and abundances. Below, we provide a brief characterisation of the Tel 2006 pollen zones from the bottom to the top of the core (Table 2).

PZ06-I (194–175 cm, ~4.25–3.83 cal ka BP) is characterised by the dominance of coniferous pollen, with prevalent indeterminate Pinaceae, *Pinus* and *Abies* pollen. Herbaceous pollen, including that of *Artemisia*, Chenopodiaceae and Cyperaceae reach 45% in this zone. Biomisation reveals taiga as a dominant biome; however, the steppe biome has high scores, with the highest point at a depth of 175 cm, where the steppe curve crosses the taiga curve (Fig. 4B). The mean scores for the taiga and steppe biomes ( $AS_t$  and  $AS_s$ ) for this zone are 16.7 and 10.13, respectively. The reconstruction of total woody coverage (WCOV) in PZ06-I demonstrates that the amount of woodland vegetation varied from 29% at the depth of 177 cm to 48% at the depth of 183 cm with a mean ( $WCOV_{av}$ ) of 39.7% (Fig. 6d).

PZ06-II (175–155 cm, ~3.83–3.39 cal ka BP) is the zone with the highest mean scores for steppe biomes throughout the core ( $AS_t = 16.45$  and  $AS_s = 12.07$ ). The pollen composition is similar to that of PZ06-I, except that the percentages of *Artemisia* and Chenopodiaceae are slightly higher. The woody coverage varies from 34% at a depth of 173 cm, to 42% at a depth of 161 cm, with  $WCOV_{av} = 37.8\%$ . Spores of *Glomus* appear in this pollen zone and then are presented more or less constantly throughout the core.

PZ06-III (155–105 cm, ~3.39–2.28 cal ka BP) is notable because of the gradual decrease in herbaceous pollen and an increase in coniferous pollen and spores of Polypodiophyta ( $AS_t = 17.67$  and  $AS_s = 9.0$ ). The quantitative estimates of woody coverage are between 34% at a depth of 113 cm and 49% at a depth of 105 cm, with  $WCOV_{av} = 43.3\%$ .

PZ06-IV (105–40 cm, ~2.28–0.83 cal ka BP (1120 CE) is characterised by the highest abundance of coniferous pollen and the lowest abundance of herbs (up to 70% and 10% at a depth of 83 cm, respectively). The mean biome scores are  $AS_t = 18.8$  and  $AS_s = 5.7$ . The percentage of woody coverage varies between 39% at a depth of 79 cm and 49% at a depth of 41 cm ( $WCOV_{av} = 46.8\%$ ).

In PZ06-V (40–0 cm, ~0.83 cal ka BP or 1120–2006 CE), coniferous pollen is predominant. Two exceptions are noted at a depth of 23–26 cm (ca 0.45–0.52 cal ka BP; 1430–1500 CE) and in the upper 2 cm of the core (from about 1960 CE onwards), when the steppe

biome scores increase. Polypodiophyta spores increase notably in this zone. Biomisation reveals biome values of  $AS_t = 17.7$  and  $AS_s = 7.0$ . The percentage woody cover varies from 42% at a depth of 24 cm, to 50% at a depth of 6 cm, with  $WCOV_{av} = 45.8\%$ . The reconstructed woody coverage at 2006 CE is 44% and is lower than the modern value observed by VSF (55%). This probably reflects the forest development in the lake's overall catchment area, including the Chulyshman River valley.

In the biome reconstruction, the taiga biome had the highest scores, with one exception at about 3.83 cal ka BP, when the steppe biome predominated (Fig. 4B). Woody coverage varied between 29% (ca. 3.88 cal ka BP) and 50.3% (ca. 1870 CE; Fig. 4).

#### 4.1.2. Tel 2001–2004

In total, 40 pollen and spore taxa were identified in the Tel 2001–2004 samples. The revealed pollen assemblages can be subdivided into three PZs (Fig. 5A).

PZ04-I (173–115 cm, ~145–0.95 cal ka BP or 500–1000 CE) is characterised by the highest abundance of coniferous pollen in the core, mainly from *Pinus s/g Haploxyton*, and the lowest abundance of herbs. The mean biome scores are  $AS_t = 15.7$  and  $AS_s = 1.1$ . PZ04-I correlates with the upper part of PZ06-IV from a depth of 70 cm (Fig. 4).

PZ04-II (115–20 cm, ~0.95–0.13 cal ka BP or 1000–1820 CE) is notable for increases in pollen from *Artemisia*, Poaceae, Chenopodiaceae, Cyperaceae and ferns. Pollen from deciduous trees and shrubs (*Betula* and *Alnus*) also increase in abundance. Biomisation reveals  $AS_t = 16.1$  and  $AS_s = 3.6$ . PZ04-II correlates with PZ06-V (Fig. 4).

PZ04-III (20–0 cm, 1820–2004 CE) is characterised by a significant increase in *Pinus s/g Haploxyton* pollen (up to 90%). However, biomisation does not show any significant changes in taiga scores ( $AS_t = 15.1$ ), whereas the steppe biome scores decreased ( $AS_s = 2.9$ ).

Biome reconstruction results show that the taiga biome has the highest scores (Fig. 5B).

#### 4.1.3. Development of an inference model

The CCA with MTWA and PANN variables had a CCA axis 1 of 0.231 and a CCA axis 2 of 0.091, which explained 11.7% and 4.6% of the variance in the data, respectively (Table 3). A set of CCAs that are constrained to individual environmental variables and Monte Carlo permutation tests, reveals that two variables explain significant proportions ( $p < 0.05$ ) of variance in the dataset: MTWA explains 5.9%, and PANN explains 3.8%.

The pollen assemblages in the subfossil dataset are strongly correlated with MTWA. The CCA with MTWA as the only constraining variable has an eigenvalue ratio of 0.55 ( $\lambda_1/\lambda_2 = 0.173/0.315$ ). The resulting two-component WA-PLS MTWA model with 204 subfossil spectra and 64 taxa yielded a high coefficient of prediction ( $r^2_{jack} = 0.82$ ), root mean-squared errors of prediction (RMSEP = 1.23) and maximum biasjack (1.38) (Fig. 7, Table 4).

## 4.2. Climate reconstruction

The application of transfer functions inferred from the training dataset resulted in MTWA estimates of July temperature fluctuations of approximately 3–4 °C during the last 4.25 ka (Fig. 6b,c). The

**Table 2**

Average values of dominant biome scores and percentages of woody cover in pollen zones of the Tel 2006 core.  $AS_t$  - average scores for taiga biome;  $AS_s$  - average scores for steppe biome;  $WCOV_{av}$  - average percentages of total woody cover; MTWA - mean July air temperature.

Pollen zone	Depth (cm)	Age	$AS_t$ scores	$AS_s$ scores	$WCOV_{av}$ %	MTWA, 0C
V	40–0	1120–2006 CE	17.7	7.0	45.8	17.04
IV	105–40	2280–830 cal yr BP	18.8	5.7	46.8	17.53
III	155–105	3390–2280 cal yr BP	17.67	9.0	43.3	17.05
II	175–155	3830–3390 cal yr BP	16.45	12.07	37.8	16.14
I	194–175	4250–3830 cal yr BP	16.7	10.13	39.7	16.89



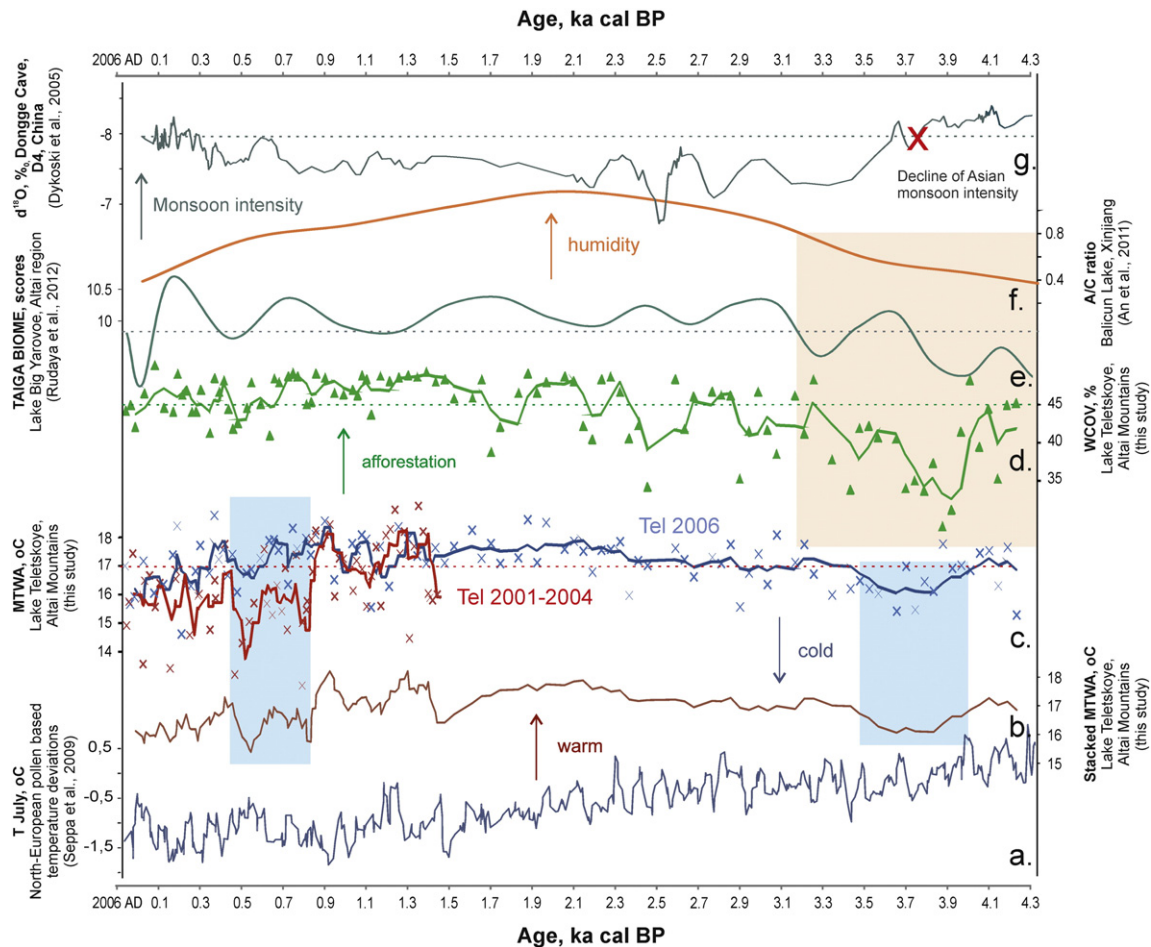


**Fig. 6.** Mid-late Holocene paleoclimate series reconstructed from Lake Teletskoye pollen data in comparison with other palaeorecords. a. T July: Linear smoothed North-European pollen based stacked July temperature deviations (Seppä et al., 2009); b. Stacked MTWA: Linear smoothed pollen-based stacked July temperatures (this study); c. MTWA: Red curve indicates reconstructed July temperature values from Tel 2001–2004; blue curve indicates Tel 2006 (this study); d. WCOV, %: Woody coverage reconstructed from pollen data of Tel 2006 (this study); e. Taiga biome curve from pollen palaeorecord of Lake Big Yarovoe, Altai region (Rudaya et al., 2012); f. A/C ratio from pollen palaeorecord of Balicun Lake, Xinjiang, China (An et al., 2011); and g.  $\delta^{18}\text{O}$  record from Dongge Cave, China, reflecting Asian monsoon intensity (Dykoski et al., 2005).

temperature curves based on the pollen data from both cores revealed similar tendencies and peaks. However, the temperature curves of the deepest Tel 2001–2004 core showed lower temperature values.

To obtain the mean July temperatures (MTWA) for the last 4.25 ka using the reconstructed temperatures from the two cores, we stacked the age models of Tel 2006 and Tel 2001–2004 into one numerical series (Fig. 6b). Periods with the lowest temperatures were reconstructed for ~3.6–3.9 cal ka BP and from 0.8 cal ka BP onwards. The lowest July temperatures occurred between 1450 and 1800 CE. A period with stable temperatures higher than modern temperatures was reconstructed for

~2.7–1.6 cal ka BP. These increased summer temperatures coincided with the maximal woody coverage and taiga biome scores (Table 2).

Goodness-of-fit statistics revealed that for the core Tel 2006, only two samples showed a 'poor' fit, two samples showed a 'very poor' fit, and 96% of the samples displayed a good fit with temperature. For the core Tel 2004, only 11% of the samples had a 'poor' fit and 89% had a 'good' fit (Fig. S1). These measures indicate that temperature reconstructions from the Tel 2004 and 2006 records are very reliable.

## 5. Discussion

The mid- to late Holocene vegetation of the north-eastern Altai Mountains, as recorded in Lake Teletskoye sediment cores, was characterised by the spread of the evergreen coniferous forest with a plant composition similar to that of the modern forest. The dominant trees were Siberian pine (*Pinus sibirica*) and Siberian fir (*Abies sibirica*). The dominance of these ecologically sensitive taxa (Shumilova, 1962) suggests relatively mild and humid climatic conditions over the last 4250 years. The studied period, called "Neoglaciation", was generally characterised by decreasing summer temperatures in the Northern Hemisphere until the beginning of the twentieth century and was terminated by 'global warming' (Wanner et al., 2011 and references therein). However, changes in the pollen percentages and the results of the numerical analysis here reveal pronounced fluctuations in climate and vegetation.

**Table 3**

Eigenvalues, taxon environmental correlations, cumulative % variance and significance of the Canonical Correspondence Analysis axes.

0.5% data set	Axis 1	Axis 2	Axis 3	Axis 4
Eigenvalues	0.231	0.091	0.059	0.225
Taxon–environment correlations	0.854	0.751	0.622	0
Cumulative % variance of taxon data	11.7	16.3	19.3	30.6
Cumulative % variance of taxon–environment relation	60.5	84.5	100.0	0
Significance (probability) of axis	0.001	0.001	0.001	0.001
Sum of all unconstrained eigenvalues	1.981			
Sum of all canonical eigenvalues	0.352			

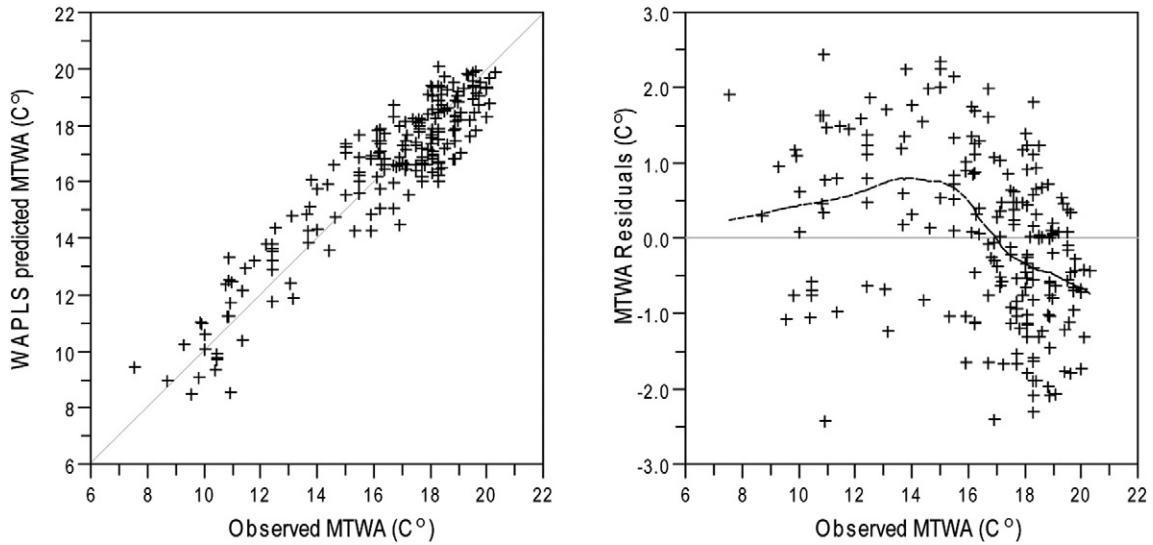


**Fig. 7.** Relationship between observed versus estimated and the residual (inferred - observed) for the pollen-inferred MTWA 2-component WA-PLS model. Trends in residuals are highlighted with a LOESS smoother (span = 0.45).

A relatively cool and dry interval occurred prior to ca. 3.5 cal ka BP. Steppe-like communities with *Artemisia*, Chenopodiaceae and Cyperaceae were widespread in the Lake Teletskoye catchment area with minimal woody cover and lower July temperatures between 3.9 and 3.6 cal ka BP. The reconstructed woody coverage varied from 29 to 35% (Fig. 6d). A modern woody coverage >65% is classified as Siberian mid-latitude zonal taiga. Areas north and south of the taiga zone have a moderate forest coverage (25–45%), suggesting greater landscape openness (Tarasov et al., 2007).

A cool and dry event at ca. 3.8 cal ka BP similar to that in the Teletskoye Lake area is recorded in many paleorecords from the Northern Hemisphere (Mayewski et al., 2004; Seppä et al., 2009; Solomina et al., 2015). Winds over the North Atlantic and Siberia were weak between 4.2 and 3.8 cal ka BP and temperatures decreased (Mayewski et al., 2004).

After ca. 3.5 cal ka BP, the area of coniferous mountain taiga significantly enlarged, with maximum of the woody coverage and taiga biome scores between 2.3 and 0.7 cal ka BP. Between 3.5 and 1.1 cal ka BP, the mean July temperatures increased by approximately 1 °C. This coincides with increased afforestation, suggesting a more humid climate. This warm and humid episode distinguishes the north-eastern Altai Mountains from Central Asia, where increasing aridity is clearly observed since ca. 5 ka BP (Chen et al., 2008 and references therein) and makes it more similar to the north-western regions. The Holocene July temperatures reconstructed from 36 paleorecords confirm a relatively warm climate interval of 3–1 cal ka BP for Northern Europe (Seppä et al., 2009; Fig. 6a). Early Holocene climatic fluctuations in northern central Asia and even in southwestern Siberia were probably influenced by Asian monsoon activity (Rudaya et al., 2009; An et al., 2011). Mid- and late Holocene climate changes are explained by the penetration of westerlies and are modulated by the North Atlantic Oscillation (An

et al., 2011) and have no connection with the late-Holocene Asian monsoon declination (Dykoski et al., 2005; Fig. 6f, g).

An et al. (2011) showed that most of the mid- to late paleorecords from northern Central Asia that are dominated by westerlies reveal a correlation between increasing aridity and increasing annual temperatures. The pollen-based reconstruction from Lake Teletskoye shows an inverse relationship. According to the results obtained from studying different natural archives, such as ice cores, sedimentary data, lake sediment palaeorecords, paleosols and pollen data, Bao et al. (2004) describe the existence of a relatively warm and humid period in northwest China between 2.2 and 1.8 cal ka BP. They explain this event by broad teleconnections within the Northern Hemisphere, which result in an enhancement of the heat contrast between mid- to high latitudes and at some lower latitudes that might strengthen the westerly circulation.

Despite the general tendency to aridisation after the Holocene climatic optimum, the pollen-based reconstruction of annual precipitation from the north Mongolian Lake Hoton-Nur (Fig. 1A), located 340 km south of Lake Teletskoye, suggests a 100 mm higher annual precipitation between 3.0 and 2.0 cal ka BP than that of today (Rudaya et al., 2009). Lake Telmen, located 760 km south-eastwards from Lake Teletskoye (Fig. 1A), showed a water level 2.7–1.3 cal ka BP that was higher than present levels and that was caused by increased precipitation (Peck et al., 2002). The pollen record from Lake Balikun, Xinjiang, China, located 960 km southward from Lake Teletskoye, shows evidence of a wet period at 3.8–2.3 cal ka BP, which is expressed as an increased *Artemisia* to Chenopodiaceae ratio (A/C ratio, Fig. 6f) following a dry event at 4.3–3.8 cal ka BP.

Increased afforestation after 3.7 cal ka BP is documented in the pollen record from Big Yarovoe Lake in the foothills of the Altai Mountains, 600 km north-west of Teletskoye Lake (Rudaya et al., 2012; Figs. 1A, 6e).

**Table 4**  
Comparison of WA and WA-PLS models for reconstructing mean July air temperature (MTWA). The best model is given in bold.

N subfossil spectra in the model	N taxa in the model	Model	$r^2_{\text{jack}}$	RMSEP (% RMSEP reduced from the previous component)	Max bias <sub>jack</sub>	
204	64	WA	Inverse	0.78	1.40	2.44
			Classical	0.78	1.50	1.09
		WA-PLS	1 component	0.78	1.35	2.31
			<b>2 component</b>	<b>0.82</b>	<b>1.23 (9.3)</b>	1.38
			3 component	0.83	1.23 (0.4)	1.48
			4 component	0.82	1.25	1.53
			5 component	0.80	1.33	1.37

Similarly, afforestation of the forest-steppe Baraba Plain, 750 km to the north-west, is recorded by a sharp increase in pine pollen dated to ca. 3.5 cal ka BP (sites Kayakskoye Zaimitsche and Suminskoye Zaimitsche; Levina et al., 1987; Klimanov et al., 1987; Fig. 1A). In the Kazakh Uplands, pine forests increased and reached their modern limit only after 2 ka BP (sites Ozerki Swamp, Lake Pashennoe, Lake Mokhovoe, Lake Karas'ye; Kremenetski et al., 1997; Tarasov et al., 1997; Fig. 1A).

Pollen records from three alpine lakes on the Ulagan Plateau (70 km south of Lake Teletskoye) suggest the dominance of mountain taiga with *Pinus sibirica*, *Pinus sylvestris* and *Larix sibirica* throughout the last 5 ka (Blyakharchuk et al., 2004; Fig. 1A). The abundances of *Picea obovata* and *Abies sibirica* pollen in these alpine lake spectra were high until ca. 1 ka BP, indicating relatively warm and humid climate conditions. During the last millennium, pollen of *Pinus sylvestris*, *Picea obovata* and *A. sibirica* decreased, whereas that of *Pinus sibirica* and *Betula* sect. *Nanae* increased, suggesting that the climate became colder and drier. Pollen data from Lake Dzhangyskol in the Kurai River basin (200 km south of Lake Teletskoye) reveal a maximal expansion of taiga in the second half of the Holocene (Blyakharchuk et al., 2008; Fig. 1A).

A short cooling interval at about 1.3–1.4 cal ka BP (550–650 CE) recorded in the Tel 2001–2004 core (Fig. 6b) was probably triggered by increased volcanic activity (e.g., the eruption in 536 CE), which is also recorded in tree-ring data and historical documents across the Northern Hemisphere (Larsen et al., 2008; Zielinski, 2000). Wanner et al. (2011) call the 300–600 CE interval “the fifth cold event of the Holocene”. This event, also known as the Dark-Age Cold Period, marks the transition between Late Antiquity and the Early Middle Ages and great human migration in Europe (Wanner et al., 2011). Schlütz and Lehmkuhl (2007) reported a cold and wet period at about 370–580 CE in the pollen record from the Tarkhata Valley in the Kurai Steppe, 240 km south of Lake Teletskoye (Fig. 1A).

A general cooling trend can be observed in the stacked July temperature curve from about 0.8–0.85 cal ka BP (1100–1150 CE). Similar trends are reflected in the Northern European and Kamchatka pollen- and chironomid-based climate reconstructions (Seppä et al., 2009; Nazarova et al., 2013; Fig. 6a).

The radiocarbon dating of trees buried by moraines reveals the advances of large glaciers located in the Altai Mountains closer to Mongolia in the thirteenth century AD, marking the Little Ice Age (LIA) onset in the Russian Altai (Agatova et al., 2012). The activation of smaller glaciers can be correlated with the coolest phase of the LIA in the second half of the fifteenth and the sixteenth centuries. Pollen data from the Chuya River basin in the southeastern part of the Russian Altai suggest that the LIA began around 1600 CE in that area (Schlütz and Lehmkuhl, 2007).

The decrease in July temperatures in the Lake Teletskoye region occurred between 1450 and 1800 CE (Fig. 6b, c), when temperatures dropped 2–3 °C below modern ones (core Tel 2001–2004). Both investigated cores showed no increase of the steppe biome scores at that time and consequently, showed no evidence of a dry LIA in the area. A humid LIA, which is typical for the Mediterranean and Western Europe, is also described in several studies in arid Central Asia (Chen et al., 2010; Yang et al., 2009).

The instrumental record of July and January temperatures from the Barnaul meteorological station spanning the last 175 years (the longest in the Altai region), shows a slight warming in winter temperatures. Our pollen-based reconstructions of July temperatures do not show any climate warming after 1850 CE; however, their resolution is not sufficiently high for comparison with the meteorological data.

## 6. Conclusion

The mid- to late Holocene (last 4.25 ka BP) vegetation dynamics in the northeastern Altai Mountains are generally characterised by the dominance of Siberian pine and Siberian fir forests. However, open steppe-like communities were widespread in the region until 3.8 ka

BP, with maximum deforestation between 3.9 and 3.6 ka BP. After ca. 3.6 ka BP, the area of dark coniferous mountain taiga significantly enlarged and approached its modern dimensions.

The climate reconstructions based on the Lake Teletskoye pollen records show that a relatively cool and dry interval occurred prior to ca. 3.5 ka BP, with lower July temperatures between 3.9 and 3.6 ka BP. In the period of ~3.5–1.6 ka BP, the mean July temperature increased by approximately 1 °C and the climate became more humid. A short period of cooling occurred between 1.4 and 1.3 ka BP. Lower July temperatures are also reconstructed for 1450–1800 CE; however, a general cooling trend that led to this minimum began about 0.85–0.8 cal ka BP (1100–1150 CE).

Supplementary data to this article can be found online at <http://dx.doi.org/10.1016/j.gloplacha.2016.04.002>.

## Acknowledgements

The pollen research was supported by grants of Russian Science Foundation (RSF) 14-50-00036. The work of N. Rudaya and L. Nazarova was sponsored by Russian Foundation for Basic Research (RFBR, 15-05-04918 A, 13-05-00621 A), German Academic Exchange Service (DAAD, Ref.325, A/05/00162) and Ministry of Education and Science of the Russian Federation, Project No. 2013-220-04-129 of the Altai State University. The work of A.A. Andreev, L. Nazarova and N. Rudaya was also partly sponsored by the Russian Government Program of Competitive Growth of Kazan Federal University. Reconstruction of woody coverage was performed by E. Novenko within the framework of the grant of the Russian Science Foundation (14-14-00956). We thank Maarten Blaauw for the assistance with Bacon 2.2 software, Richard Telford for valuable advices in multivariate statistics, Heikki Seppä for digital dataset of Northern Hemisphere temperatures, and Peter Hindmarch for English correction. Our sincere thanks are given to the manuscript reviewers Stefanie Müller and Sergey Krivonogov for their valuable comments.

## References

- Agatova, A.R., Nazarova, A.N., Nepop, R.K., Rodnight, H., 2012. Holocene glacier fluctuations and climate changes in the southeastern part of the Russian Altai (South Siberia) based on a radiocarbon chronology. *Quat. Sci. Rev.* 43, 74–93. <http://dx.doi.org/10.1016/j.quascirev.2012.04.012>.
- Altman, D., Bland, J.M., 1983. Measurement in medicine: the analysis of method comparison studies. *The Statistician* 32, 307–317.
- An, C.-B., Lu, Y., Zhao, J., Tao, S., Dong, W., Li, H., Jin, M., Wang, Z., 2011. A high-resolution record of Holocene environmental and climatic changes from Lake Balikun (Xinjiang, China): Implications for central Asia. *The Holocene* 22 (1), 43–52. <http://dx.doi.org/10.1177/0959683611405244>.
- Andreev, A., Pierau, R., Kalugin, I., Daryin, A., Smolyaninova, L., Diekmann, B., 2007. Environmental changes in the northern Altai during the last millennium documented in Lake Teletskoye pollen record. *Quat. Res.* 67, 394–399. <http://dx.doi.org/10.1016/j.yqres.2006.11.004>.
- Atlas of geological maps of Central Asia and adjacent areas, 2008. In: Daukeev, S.Z., Kim, B.C., Tingdong, L., Petrov, O.V., Tomurtogoo, O. (Eds.), Geological Publishing House.
- Bao, Y., Braeuning, A., Yafeng, S., Fahu, C., 2004. Evidence for a late Holocene warm and humid climate period and environmental characteristics in the arid zones of north-west China during 2.2–1.8 kyr B.P. *Journal of Geophysical Research* 109, D02105. <http://dx.doi.org/10.1029/2003JD003787>.
- Barley, E.M., Walker, I.R., Kurek, J., Cwynar, L.C., Mathewes, R.W., Gajewski, K., Finney, B.P., 2006. A northwest North American training set: distribution of freshwater mides in relation to air temperature and lake depth. *Journal of Paleolimnology* 36, 295–314. <http://dx.doi.org/10.1007/s10933-006-0014-6>.
- Birks, H.J.B., 1995. Quantitative palaeoenvironmental reconstructions. In: Maddy, D., JS, B. (Eds.), *Statistical Modelling of Quaternary Science Data*. Technical Guide 5, Quaternary Research Association, Cambridge, pp. 161–254.
- Birks, H.J.B., 1998. Numerical tools in paleolimnology progress, potential, and problems. *J. Paleolimnol.* 20, 307–332.
- Birks, H.J.B., 2010. Numerical methods for the analysis of diatom assemblage data. In: Smol, J.P., Stoermer, E.F. (Eds.), *The Diatoms: Application for the Environmental and Earth Sciences*, second ed. Cambridge University Press, Cambridge, pp. 23–54.
- Birks, H.J.B., Juggins, S., Line, J.M., 1990. Lake surface-water chemistry reconstructions from palaeolimnological data. In: Mason, B. (Ed.), *The Surface Water Acidification Programme*. Cambridge University Press, Cambridge, pp. 301–313.
- Blaauw, M., Christen, J.A., 2011. Flexible paleoclimate age-depth models using an autoregressive gamma process. *Bayesian Anal.* 6, 457–474. <http://dx.doi.org/10.1214/11-BA618>.



- Blyakharchuk, T.A., Wright, H.E., Borodavko, P.S., van der Knaap, W.O., Ammann, B., 2004. Late-glacial and Holocene vegetational changes on the Ulagan high-mountain plateau, Altai Mountains, southern Siberia. *Palaeogeogr. Palaeoclimatol. Palaeoecol.* 209, 259–279. <http://dx.doi.org/10.1016/j.palaeo.2004.02.011>.
- Blyakharchuk, T.A., Wright, H.E., Borodavko, P.S., van der Knaap, W.O., Ammann, B., 2007. Late Glacial and Holocene vegetational history of the Altai Mountains (southwestern Tuva Republic, Siberia). *Palaeogeogr. Palaeoclimatol. Palaeoecol.* 245, 518–534. <http://dx.doi.org/10.1016/j.palaeo.2006.09.010>.
- Blyakharchuk, T.A., Wright, H.E., Borodavko, P.S., van der Knaap, W.O., Ammann, B., 2008. The role of Pingos in the development of the Dzhangyskol lake–Pingo complex, central Altai Mountains, southern Siberia. *Palaeogeogr. Palaeoclimatol. Palaeoecol.* 254 (4), 404–420. <http://dx.doi.org/10.1016/j.palaeo.2007.09.015>.
- Box, E.O., 1996. Plant functional types and climate at the global scale. *J. Vegetation Science* 7, 309–320.
- Bradshaw, R.H.W., Webb III, T., 1985. Relationships between contemporary pollen and vegetation data from Wisconsin and Michigan, USA. *Ecology* 66, 721–737.
- Chen, F., Yu, Y., Yang, M., Ito, E., Wang, S., Madsen, D.B., Huang, X., Zhao, Y., Sato, T., Birks, H.J.B., Boomer, I., Chen, J., An, C., Wünnemann, B., 2008. Holocene moisture evolution in arid central Asia and its out-of-phase relationship with Asian monsoon history. *Quat. Sci. Rev.* 27, 351–364.
- Chen, F.-H., Chen, J.-H., Holmes, J., Boomer, I., Austin, P., Gates, J.B., Wang, N.-L., Brooks, S.J., Zhang, J.-W., 2010. Moisture changes over the last millennium in arid central Asia: a review, synthesis and comparison with monsoon region. *Quat. Sci. Rev.* 29 (7–8), 1055–1068. <http://dx.doi.org/10.1016/j.quascirev.2010.01.005>.
- Colman, S.M., Jones, G.A., Rubin, M., King, J.W., Peck, J.A., Orem, W.H., 1996. AMS radiocarbon analyses from Lake Baikal, Siberia: challenges of dating sediments from a large, oligotrophic lake. *Quat. Sci. Rev.* 15, 669–684.
- Derevianko, A.P., Shunkov, M.V., Agadjanjan, A.K., Baryshnikov, G.F., Malaeva, E.M., Ulianov, V.A., Kulik, N.A., Postnov, A.V., Anokin, A.A., 2003. Prirodnyaya Sreda I Chelovek V Paleolite Gornogo Altaya. I AET SO RAN, Novosibirsk (in Russian).
- Dykoski, C.A., Edwards, R.L., Cheng, H., Yuan, D., Cai, Y., Zhang, M., Lin, Y., Qiang, J., An, Z., Revenaugh, J., 2005. A high-resolution absolute-dated Holocene and deglacial Asian monsoon record from Dongge Cave, China. *Earth Planet. Sci. Lett.* 233, 71–86.
- Ermakov, N.B., 2003. Raznoobrazie Borealnoi Rastitelnosti Severnoi Asii. Gemiborealnyye lesa. Klassifikatsiya i ordinatsiya, Novosibirsk (in Russian).
- Faegri, K., Iversen, J., 1989. *Textbook of Pollen Analysis*. John Wiley and Sons, Chichester.
- Grimm, E., 1987. CONISS: A FORTRAN 77 program for stratigraphically constrained cluster analysis by the methods of incremental sum of squares. *Comput. Geosci.* 13, 13–15.
- Grimm, E., 2004. Tilia software 2.0.2. Illinois State Museum Research and Collection Center, Springfield.
- Guiot, J., 1990. Methodology of the last climatic cycle reconstruction in France from pollen data. *Palaeogeogr. Palaeoclimatol. Palaeoecol.* 80, 49–69. [http://dx.doi.org/10.1016/0031-0182\(90\)90033-4](http://dx.doi.org/10.1016/0031-0182(90)90033-4).
- Gunin, P.D., Vostokova, E.A., Dorofeyuk, N.I., Tarasov, P.E., Black, C.C. (Eds.), 1999. *Vegetation Dynamics of Mongolia*. Kluwer Academic Publishers, Dordrecht.
- Hansen, M., DeFries, R.S., Townshend, J.R.G., Carroll, M., Dimiceli, C., Sohlberg, R.A., 2003. Global percent tree cover at a spatial resolution of 500 meters: first results of the MODIS vegetation continuous fields algorithm. *Earth Interactions* 7 (10), 1–15.
- Hellman, S.E.V., Gaillard, M.-J., Broström, A., Sugita, S., 2008. Effects of the sampling design and selection of parameter values on pollen-based quantitative reconstructions of regional vegetation: a case study in southern Sweden using the REVEALS model. *Vegetation History and Archaeobotany* 17, 445–459.
- Hill, M.O., Gauch, H.G., 1980. Detrended correspondence analysis – an improved ordination technique. *Vegetatio* 42, 47–58.
- Juggins, S., 2007. C2 Version 1.5 User guide. Software for Ecological and Palaeoecological Data Analysis and Visualisation. Newcastle University, Newcastle upon Tyne, UK.
- Juggins, S., Birks, H.J.B., 2012. Chapter 14: Quantitative environmental reconstructions from biological data. In: HJB, B., AF, L., Juggins, S., JP, S. (Eds.), *Tracking Environmental Change Using Lake Sediments Data Handling and Numerical Techniques Vol 5*. Springer, Dordrecht.
- Kalugin, I., Daryin, A., Smolyaninova, L., Andreev, A., Diekmann, B., Khlystov, O., 2007. 800-yr-long records of annual air temperature and precipitation over southern Siberia inferred from Teletskoye Lake sediments. *Quat. Res.* 67 (3), 400–410. <http://dx.doi.org/10.1016/j.yqres.2007.01.007>.
- Kalugin, I., Selegei, V., Goldberg, E., Seret, G., 2005. Rhythmic fine-grained sediment deposition in Lake Teletskoye, Altai, Siberia, in relation to regional climate change. *Quat. Int.* 136, 5–13. <http://dx.doi.org/10.1016/j.quaint.2004.11.003>.
- Kalugin, I.A., Daryin, A.V., Babich, V.V., 2009. Reconstruction of annual air temperatures for three thousand years in altai region by lithological and geochemical indicators in teletskoe lake sediments. *Dokl. Earth Sci.* 426 (1), 681–684.
- Klimanov, V.A., Levina, T.P., Orlova, L.A., Panychev, V.A., 1987. *Izmenenie Klimata na Territorii Barabinskoi Ravniny V Subatlaticheskom Periode Golotsena Po Dannym Izuicheniya Torfyannika Suminskogo Zaimitscha. Regionalnaya geokhronologiya Sibiri i Dalnego Vostoka. Novosibirsk, In*, pp. 143–149 (in Russian).
- Kremenetski, V., Tarasov, P., Cherkinsky, E., 1997. Postglacial development of Kazakhstan pine forests. *Geog. Phys. Quatern.* 51, 391–404.
- Kuminova, A.V., 1960. *Rastitelnyy Pokrov Altaya Novosibirsk*. (in Russian).
- Larsen, L.B., Vinther, B.M., Briffa, K.R., Melvin, T.M., Clausen, H.B., Jones, P.D., Siggaard-Andersen, M.L., Hammer, C.U., Eronen, M., Grudd, H., Gunnarsson, B.E., Hantemirov, R.M., Naurzbaev, M.M., Nicolussi, K., 2008. New ice core evidence for a volcanic cause of the 536 CE dust veil. *Geophysical Research Letters* 35, L04708. <http://dx.doi.org/10.1029/2007GL032450>.
- Lavrenko, E.M., 2000. *Stepi SSSR. Izbrannyye trudy, Saint-Petersburg* (in Russian).
- Levina, T.P., Orlova, L.A., Panychev, V.A., Ponomareva, E.A., 1987. *Radiokhronometriya I Pylzevaya Stratigrafiya Golozenovogo Torfyannika Kayakskogo Zaimitscha (Barabinskaya Lesostep). Regionalnaya geokhronologiya Sibiri i Dalnego Vostoka, Novosibirsk*, pp. 136–143 (in Russian).
- Mayewski, P.A., Rohling, E.E., Stager, J.C., Karlén, W., Maasch, K.A., Meeker, L.D., Meyerson, E.A., Gasse, F., van Kreveld, S., Holmgren, K., Lee-Thorp, J., Rosqvist, G., Rack, F., Staubwasser, M., Schneider, R.R., Steig, E.J., 2004. Holocene climate variability. *Quat. Res.* 62 (3), 243–255. <http://dx.doi.org/10.1016/j.yqres.2004.07.001>.
- Moreton, S.G., Roseqvist, G.C., Davies, S.J., Bentley, M.J., 2004. Radiocarbon reservoir ages from freshwater lakes, south Georgia, sub-Antarctic: modern analogues from particulate organic matter and surface sediments. *Radiocarbon* 46 (2), 621–626.
- Nazarova, L., de Hoog, V., Hoff, U., Dirksen, O., Diekmann, B., 2013. Late Holocene climate and environmental changes in Kamchatka inferred from the subfossil chironomid record. *Quat. Sci. Rev.* 67, 81–92. <http://dx.doi.org/10.1016/j.quascirev.2013.01.018>.
- New, M., Lister, D., Hulme, M., Makin, I., 2002. A high-resolution data set of surface climate over global land areas. *Clim. Res.* 21, 1–25.
- Novenko, E.Y., Ereemeeva, A.P., Chepurina, A.A., 2014. Reconstruction of Holocene vegetation, tree cover dynamics and human disturbances in central European Russia, using pollen and satellite data sets. *Vegetation History and Archaeobotany* 23, 109–119. <http://dx.doi.org/10.1007/s00334-013-0418-y>.
- Overland, J.E., Wang, M., 2005. The Arctic climate paradox: the recent decrease of the Arctic oscillation. *Geophys. Res. Lett.* 32, 1–5.
- Overpeck, J.T., Webb III, T., Prentice, I.C., 1985. Quantitative interpretation of fossil pollen spectra: dissimilarity coefficients and the method of modern analogs. *Quat. Res.* 23, 87–108.
- Peck, J., Khosbayan, P., Fowell, S., Pearce, R., Ariunbileg, S., Hansen, B., Soninkhishig, N., 2002. Mid to late Holocene climate change in north central Mongolia as recorded in the sediments of Lake Telmen. *Palaeogeogr. Palaeoclimatol. Palaeoecol.* 183, 135–153.
- Polosmak, N., 2001. *Vsadniki Ukoka*. Infolio-Press, Novosibirsk (in Russian).
- Prentice, I.C., Guiot, J., Huntley, B., Jolly, D., Cheddadi, R., 1996. Reconstructing biomes from palaeoecological data: a general method and its application to European pollen data at 0 and 6 ka. *Clim. Dyn.* 12, 185–194.
- Prokopenko, A.A., Khursevich, G.K., Bezrukova, E.V., Kuzmin, M.I., Boes, X., Williams, D.F., Fedenya, S.A., Kulagina, N.V., Letunova, P.P., Abzaeva, A.A., 2007. Palaeoenvironmental proxy records from Lake Hovsgol, Mongolia, and a synthesis of Holocene climate change in the Lake Baikal watershed. *Quat. Res.* 68, 2–17. <http://dx.doi.org/10.1016/j.yqres.2007.03.008>.
- Core Team, R., 2012. *R: A Language and Environment for Statistical Computing*. R Foundation for Statistical Computing, Vienna.
- Rudaya, N., 2013. Environmental conditions during the early human settlement of Chagyrskaya Cave (Altai). *Archaeology Ethnology and Anthropology of Eurasia* 41, 45–54. <http://dx.doi.org/10.1016/j.aee.2013.07.004>.
- Rudaya, N., Nazarova, L., Nourgaliev, D., Palagushkina, O., Papin, D., Frolova, L., 2012. Middle-late Holocene environmental history of Kulunda, southwestern Siberia: vegetation, climate and humans. *Quat. Sci. Rev.* 48, 32–42. <http://dx.doi.org/10.1016/j.quascirev.2012.06.002>.
- Rudaya, N., Tarasov, P., Dorofeyuk, N., Solovieva, N., Kalugin, I., Andreev, A., Daryin, A., Diekmann, B., Riedel, F., Tserendash, N., Wagner, M., 2009. Holocene environments and climate in the Mongolian Altai reconstructed from the Hoton-Nur pollen and diatom records: a step towards better understanding climate dynamics in Central Asia. *Quat. Sci. Rev.* 28, 540–554. <http://dx.doi.org/10.1016/j.quascirev.2008.10.013>.
- Rusanov, G.G., Orlova, L.A., 2013. *Radiouglerodnyye datirovki (SOAN) Gornogo Altaya i predaltayskoy ravniny. Biisk: FBGOU VPO "AGA"* (in Russian).
- Schlütz, F., Lehmkuhl, F., 2007. Climatic change in the Russian Altai, southern Siberia, based on palynological and geomorphological results, with implications for climatic teleconnections and human history since the middle Holocene. *Vegetation History and Archaeobotany* 16, 101–118.
- Selegei, V.V., Selegei, T.V., 1978. *Teletskoye Lake. Gydrometeoizdat, Leningrad* (in Russian).
- Seleznev, V.S., Nikolaev, V.G., Buslov, M.M., Babushkin, S.M., Larkin, G.V., Evdokimov, A.A., 1995. *Struktura osadochnuh otlozhenii Teletskogo ozera po dannym napravlenogo odnokanalnogo seismoprofilirovaniya. Geol. Geofiz.* 10, 123–142 (in Russian).
- Seppä, H., Bjune, A.E., Telford, R.J., Birks, H.J.B., Veski, S., 2009. Last nine-thousand years of temperature variability in northern Europe. *Clim. Past* 5 (3), 523–535. <http://dx.doi.org/10.5194/cp-5-523-2009>.
- Shumilova, L.V., 1962. *Botanicheskaya Geografiya Sibiri Tomsk*. (in Russian).
- Sokal, R.R., Rohlf, F.J., 1995. *Biometry: The Principles and Practice of Statistics in Biological Research*. W. H. Freeman and Co, New York.
- Solomina, O.N., Bradley, R.S., Hodgson, D.A., Ivy-Ochs, S., Jomelli, V., Mackintosh, A.N., Nesje, A., Owen, L.A., Wanner, H., Wiles, G.C., Young, N.E., 2015. Holocene glacier fluctuations. *Quat. Sci. Rev.* 111, 9–34. <http://dx.doi.org/10.1016/j.quascirev.2014.11.018>.
- Takhtajan, A.L., 1986. *Floristic Regions of the World*. Berkeley.
- Tarasov, P., Williams, J.W., Andreev, A., Nakagawa, T., Bezrukova, E., Herzschuh, U., Igarashi, Y., Müller, S., Werner, K., Zheng, Z., 2007. Satellite- and pollen-based quantitative woody cover reconstructions for northern Asia: Verification and application to late-quaternary pollen data. *Earth Planet. Sci. Lett.* 264, 284–298.
- Tarasov, P., Dorofeyuk, N., Metel'tseva, E., 2000. Holocene vegetation and climate changes in Hoton-Nur basin, northwest Mongolia. *Boreas* 29, 117–126.
- Tarasov, P., Jolly, D., Kaplan, J., 1997. A continuous late glacial and Holocene record of vegetation changes in Kazakhstan. *Palaeogeogr. Palaeoclimatol. Palaeoecol.* 136, 281–292.
- ter Braak, C.J.F., 1990. Update notes: CANOCO Version 3.10. *Agricultural Mathematics Group, Wageningen*.
- ter Braak, C.J.F., 1995. *Ordination*. In: Jongman, R.H.G., ter Braak, C.J.F., van Tongeren, O.F.R. (Eds.), *Data Analysis in Community and Landscape Ecology*. Cambridge University Press, Cambridge, pp. 69–173.

- ter Braak, C.J.F., Juggins, S., 1993. Weighted averaging partial least squares regression (WA-PLS): an improved method for reconstructing environmental variables from species assemblages. *Hydrobiologia* 269 (270), 485–502.
- ter Braak, C.J.F., Looman, C.W.N., 1986. Weighted averaging, logistic regression and the Gaussian response model. *Vegetation* 65, 3–11.
- ter Braak, C.J.F., Prentice, I.C., 1988. A theory of gradient analysis. *Adv. Ecol. Res.* 18, 271–317.
- ter Braak, C.J.F., Šmilauer, P., 2002a. *CANOCO Reference Manual and CanoDraw for Windows User's Guide: Software for Canonical Community Ordination (version 4.5)*. Microcomputer Power, Ithaca, NY.
- ter Braak, C.J.F., Šmilauer, P., 2002b. *CANOCO for Windows: software for community ordination (version 4.5)*. Microcomputer Power, Ithaca New York.
- Wang, Y., Herzschuh, U., Shumilovskikh, L.S., Mischke, S., Birks, H.J.B., Wischniewski, J., Böhner, J., Schlütz, F., Lehmkuhl, F., Diekmann, B., Wünnemann, B., Zhang, C., 2014. Quantitative reconstruction of precipitation changes on the NE Tibetan plateau since the last glacial maximum – extending the concept of pollen source area to pollen-based climate reconstructions from large lakes. *Clim. Past* 10, 21–39.
- Wanner, H., Solomina, O., Grosjean, M., Ritz, S.P., Jetel, M., 2011. Structure and origin of Holocene cold events. *Quat. Sci. Rev.* 30, 3109–3123.
- Watanabe, T., Nakamura, T., Nara, F.W., Kakegawa, T., Horiuchi, K., Senda, R., Oda, T., Nishimura, M., Matsumoto, G.I., Kawai, T., 2009. High-time resolution AMS <sup>14</sup>C data sets for Lake Baikal and Lake Hovsgol sediment cores: Changes in radiocarbon age and sedimentation rates during the transition from the last glacial to the Holocene. *Quat. Int.* 205, 12–20.
- Yang, B., Wang, J., Bräuning, A., Dong, Z., Esper, J., 2009. Late Holocene climatic and environmental changes in arid central Asia. *Quat. Int.* 194, 68–78. <http://dx.doi.org/10.1016/j.quaint.2007.11.020>.
- Zhou, A., He, Y., Wu, D., Zhang, X., Zhang, C., Liu, Z., Yu, J., 2015. Changes in the radiocarbon reservoir age in Lake Xingyun, Southwestern China during the Holocene. *PLoS One* 10 (3), e0121532. <http://dx.doi.org/10.1371/journal.pone.0121532>.
- Zielinski, G.A., 2000. Use of paleo-records in determining variability within the volcanism-climate system. *Quat. Sci. Rev.* 19, 417–438.